Acta Cryst. (1977). B33, 763–770

The Crystal Structures of the Low- and High-Temperature Modifications of Potassium 7,7,8,8-Tetracyanoquinodimethanide

BY M. KONNO, T. ISHII* AND Y. SAITO

The Institute for Solid State Physics, The University of Tokyo, Roppongi-7, Minato-ku, Tokyo 106, *Japan*

(*Received* 26 *July* 1976; *accepted* 10 *August* 1976)

Crystals of K^+TCNQ^- undergo a first-order phase transition at about 122 °C. The crystal structures of the low- and high-temperature modifications have been determined by X-ray diffraction. Crystals of the low-temperature phase are monoclinic with space group $P2_1/n$, $a = 7{\cdot}0835\ (7)$, $b = 17{\cdot}773\ (3)$, $c = 17{\cdot}859\ (4)$ Å, $\beta = 94{\cdot}95\ (1)°$ and $Z = 8$. Those of the high-temperature phase are monoclinic with space group $P2_1/c$, $a = 3{\cdot}587\ (3)$, $b = 12{\cdot}676\ (5)$, $c = 12{\cdot}614\ (5)$ Å, $\beta = 96{\cdot}44\ (3)°$ and $Z = 2$. Refinement by the block-diagonal least-squares procedure followed by full-matrix least-squares refinement reduced the R values to 0·044 for 2188 observed reflexions and 0·052 for 367 observed reflexions for the low- and high-temperature modifications respectively. In the low-temperature phase, $TCNQ^-$ anions are stacked face-to-face to form columns along the a axis with alternating interplanar spacings of 3·237 and 3·567 Å, indicating the presence of $TCNQ^-$ dimers, while $TCNQ^-$ anions are arranged with an equal interplanar spacing of 3·479 Å above the transition temperature. A K^+ ion is at the centre of a distorted cube consisting of eight N atoms of different $TCNQ^-$ anions.

Introduction

Recently a number of studies have been reported on the phase transitions of organic radical salts with one-dimensional systems (de Boer & Vos, 1972; Comès, Lambert, Launois & Zeller, 1973; Konno & Saito, 1975; Denoyer, Comès, Garito & Heeger, 1975). TCNQ radical salts with high electrical conductivities have particularly aroused considerable interest. Alkali$^+$ $TCNQ^-$ salts, except Li, undergo the phase transition. The crystal structures of the low- and high-temperature phases of Na^+TCNQ^- have been determined (Konno & Saito, 1974, 1975) and it was revealed that the dimeric structure of the TCNQ column transforms into a monomeric one on passing through the transition temperature.

Anderson & Fritchie (1963) determined the structure of the low-temperature phase of K^+TCNQ^-. Since they neglected all the weak reflexions with h odd, what they determined was the 'average structure' and no conclusion could be drawn as to whether or not the TCNQ columns contain dimers. The crystal structure of the low-temperature phase has now been determined completely, based on all the observed reflexions including weak 'odd' reflexions. In the present paper, the structures of the low- and high-temperature modifications of K^+TCNQ^- are reported.

* Present address: Department of Chemistry, Chiba Institute of Technology, Narashino, Chiba 275, Japan.

Experimental and structure determination

Low-temperature phase

Crystals of K^+TCNQ^- were kindly provided by Dr Sakai of this Institute. All the crystal specimens were found to be twinned to form quadruplets around the a axis owing to the approximate tetragonal geometry in the (100) plane. A crystal with dimensions 0·13 × 0·22 × 0·31 mm was used for data collection. It was mounted on an automatic four-circle diffractometer with the a axis nearly parallel to the φ axis of the goniostat. Reflexions were measured to a maximum 2θ value of 55° with graphite-monochromated Mo $K\alpha$ radiation.

Table 1. *The crystallographic data of the low- and high-temperature modifications of* K^+TCNQ^-

$K(C_{12}H_4N_4)$, F.W. 243·3

	Low-temperature modification (25 °C)	High-temperature modification (140 °C)
	Monoclinic	Monoclinic
Space group	$P2_1/n$	$P2_1/c$
a	7·0835 (7) Å	3·587 (3) Å
b	17·773 (3)	12·676 (5)
c	17·859 (4)	12·614 (5)
β	94·95 (1)°	96·44 (3)°
U	2239·9 (6) Å^3	570·0 (6) Å^3
Z	8	2
D_m	1·442 g cm^{-3}	
D_x	1·443 g cm^{-3}	1·417 g cm^{-3}

Measurements of three standard reflexions were repeated every 50 reflexions. The ω-scan technique was employed because of twinning. If two neighbouring reflexions overlapped, the intensities of the two reflexions were measured at the same time and were separated by the same procedure as described in a previous paper (Konno & Saito, 1974). The $0kl$ reflexions, however, could not be separated owing to an approximate tetragonal symmetry on the (100) plane. In total, 2188 independent reflexions with $|F| \geq 3\sigma$ were collected. The density of the crystal was measured by flotation. The crystal data are given in Table 1.

The atomic parameters of the average structure determined by Anderson & Fritchie (1963) were refined by block-diagonal least-squares calculations on the basis of all the observed reflexions with h even to an R value of 0·12. The deviations of the TCNQ units from the average structure were deduced from negative peaks on Patterson maps calculated by employing the h-odd reflexions. The atomic parameters thus deduced were refined by assuming anisotropic thermal motion for all the non-hydrogen atoms and isotropic thermal motion for the H atoms. The last cycle was refined by full-matrix least squares. At this stage the R value became 0·044 for the 2188 observed reflexions. Unit weight was given to all the reflexions. The atomic scattering factors were taken from *International Tables for X-ray Crystallography* (1962). The scattering curve for

Table 2. *Atomic parameters for the low-temperature modification*

(*a*) Non-hydrogen parameters ($\times 10^4$). The U_{ij} values refer to the expression:

$$\exp[-2\pi^2(U_{11}h^2a^{*2} + U_{22}k^2b^{*2} + U_{33}l^2c^{*2} + 2U_{12}hka^*b^* + 2U_{13}hla^*c^* + 2U_{23}klb^*c^*)].$$

Here and elsewhere in this paper the estimated standard deviations in the last figure are given in parentheses.

	x	y	z	U_{11}	U_{22}	U_{33}	U_{12}	U_{13}	U_{23}
K(1)	593 (1)	2459 (1)	2555 (1)	313 (5)	284 (4)	286 (5)	7 (4)	59 (4)	0 (4)
K(2)	5577 (1)	2527 (1)	2517 (1)	335 (5)	282 (5)	288 (6)	−20 (4)	77 (4)	3 (4)
C(1)	2644 (6)	17 (2)	748 (2)	272 (23)	264 (20)	258 (21)	−5 (14)	36 (17)	−11 (16)
C(2)	3094 (6)	674 (2)	361 (2)	388 (25)	210 (19)	263 (23)	−36 (16)	2 (17)	−19 (17)
C(3)	3079 (6)	678 (2)	−410 (2)	409 (25)	177 (18)	274 (23)	−38 (16)	18 (18)	22 (16)
C(4)	2625 (6)	19 (2)	−837 (2)	267 (22)	265 (20)	270 (22)	−3 (15)	27 (18)	32 (17)
C(5)	2145 (6)	−638 (2)	−445 (3)	405 (25)	168 (19)	340 (26)	−20 (16)	59 (19)	−36 (17)
C(6)	2155 (6)	−639 (2)	321 (2)	395 (25)	194 (19)	305 (27)	−8 (16)	77 (19)	16 (17)
C(7)	2666 (6)	19 (2)	1545 (2)	357 (25)	245 (19)	245 (20)	4 (15)	63 (18)	−28 (16)
C(8)	2620 (6)	19 (2)	−1634 (2)	340 (23)	223 (18)	280 (21)	−2 (14)	37 (18)	25 (16)
C(9)	2981 (5)	688 (2)	−2029 (2)	351 (24)	254 (20)	234 (22)	5 (16)	4 (17)	−3 (16)
C(10)	2211 (6)	−629 (2)	−2059 (2)	383 (25)	275 (21)	249 (23)	0 (16)	22 (18)	42 (17)
C(11)	2217 (6)	−640 (2)	1946 (2)	354 (25)	265 (20)	278 (24)	−1 (16)	68 (19)	−13 (17)
C(12)	2986 (6)	680 (2)	1976 (2)	366 (25)	246 (20)	262 (23)	−1 (16)	68 (18)	6 (17)
N(1)	3250 (6)	1241 (2)	−2335 (2)	579 (26)	324 (21)	365 (24)	22 (17)	59 (19)	97 (18)
N(2)	1880 (6)	−1173 (2)	−2397 (2)	701 (30)	339 (22)	331 (23)	−128 (18)	47 (20)	−54 (18)
N(3)	1885 (6)	−1174 (2)	2269 (2)	624 (27)	319 (21)	402 (25)	−46 (17)	76 (19)	104 (18)
N(4)	3236 (6)	1221 (2)	2316 (2)	615 (28)	293 (20)	434 (26)	−12 (17)	109 (20)	−67 (18)
C(13)	2461 (5)	−745 (2)	4982 (2)	258 (21)	272 (19)	235 (23)	−19 (15)	40 (15)	25 (16)
C(14)	2251 (6)	−325 (2)	5647 (2)	373 (25)	298 (22)	225 (23)	−4 (17)	51 (18)	13 (17)
C(15)	2421 (6)	435 (2)	5657 (3)	384 (24)	330 (22)	217 (24)	23 (17)	72 (18)	13 (17)
C(16)	2823 (6)	844 (2)	5008 (2)	318 (24)	240 (20)	240 (24)	35 (15)	41 (17)	20 (15)
C(17)	3015 (6)	426 (2)	4342 (3)	443 (27)	263 (21)	229 (24)	−13 (17)	97 (19)	16 (17)
C(18)	2852 (6)	−339 (2)	4331 (3)	377 (26)	301 (22)	247 (25)	1 (17)	66 (19)	18 (18)
C(19)	2295 (5)	−1540 (2)	4966 (2)	340 (23)	276 (20)	213 (22)	−18 (16)	43 (16)	16 (15)
C(20)	3011 (5)	1637 (2)	5016 (2)	356 (23)	268 (20)	221 (23)	9 (16)	53 (17)	35 (15)
C(21)	2857 (6)	2062 (2)	5680 (3)	393 (26)	261 (20)	286 (26)	1 (16)	81 (19)	41 (17)
C(22)	3284 (6)	2048 (2)	4357 (2)	402 (25)	264 (20)	204 (24)	34 (16)	−8 (17)	13 (17)
C(23)	2344 (6)	−1955 (2)	4290 (2)	404 (25)	271 (21)	233 (25)	−53 (16)	18 (18)	8 (17)
C(24)	1926 (6)	−1959 (2)	5620 (3)	343 (24)	289 (21)	267 (25)	8 (16)	45 (17)	−12 (18)
N(5)	2750 (6)	2394 (2)	6224 (2)	775 (30)	308 (21)	365 (24)	6 (19)	184 (20)	−45 (19)
N(6)	3489 (5)	2359 (2)	3809 (2)	559 (25)	403 (22)	324 (22)	41 (18)	79 (18)	50 (18)
N(7)	2369 (5)	−2279 (2)	3740 (2)	624 (27)	374 (21)	299 (22)	−59 (18)	56 (18)	−67 (18)
N(8)	1629 (6)	−2287 (2)	6143 (2)	661 (28)	352 (21)	328 (23)	−48 (18)	128 (19)	57 (18)

(*b*) Hydrogen coordinates ($\times 10^3$) and isotropic temperature factors

	x	y	z	B (Å^2)		x	y	z	B (Å^2)
H(2)	366 (7)	112 (3)	68 (3)	5·5 (1·4)	H(14)	195 (6)	−62 (3)	612 (3)	3·5 (1·0)
H(3)	348 (5)	113 (2)	−65 (2)	1·6 (0·8)	H(15)	235 (6)	71 (3)	614 (3)	4·0 (1·1)
H(5)	174 (6)	−109 (3)	−75 (3)	3·3 (1·0)	H(17)	328 (6)	72 (3)	388 (3)	3·5 (1·0)
H(6)	182 (6)	−110 (3)	59 (3)	2·8 (0·9)	H(18)	292 (6)	−58 (3)	386 (3)	3·2 (1·0)

H was that listed by Stewart, Davidson & Simpson (1965). The final atomic parameters are given in Table 2.

High-temperature phase

The crystal specimens were heated in a stream of electrically heated air. Preliminary oscillation and Weissenberg photographs around the a axis were taken at about 140 °C. It was observed that weak reflexions with h odd in the low-temperature phase disappeared completely. These photographs of the high-temperature phase indicated that it is monoclinic and that its unit-cell edges (a', b', c') are related to those of the low-temperature phase (a,b,c) as follows: $\mathbf{a}' = \mathbf{a}/2$, $\mathbf{b}' = (\mathbf{b} + \mathbf{c})/2$, $\mathbf{c}' = (-\mathbf{b} + \mathbf{c})/2$.

Intensity data were collected on a manual four-circle diffractometer with a crystal of dimensions 0·14 × 0·24 × 0·32 mm cut from the same specimen used for the intensity measurement of the low-temperature modification. It was mounted with the a axis nearly parallel to the φ axis of the goniostat. The ω-scan technique was employed because the crystal specimen consisted of quadruplets similar to those of the low-temperature phase. Three standard reflexions were measured every three hours. 367 independent reflexions with $|F| \geq 3\sigma$ in the range $2\theta \leq 40°$ were collected and used for structure determination. All the $0kl$ reflexions were excluded, since they could not be separated owing to the formation of quadruplets. The intensities were corrected for Lorentz and polarization factors but no correction for absorption was made for the two modifications. Table 1 also lists the crystal data of the high-temperature modification.

The starting coordinates of the high-temperature phase could be readily deduced from the atomic coordinates of the low-temperature phase. Several cycles of refinement by the block-diagonal least-squares procedure followed by a few cycles of full-matrix least-squares refinement reduced R to 0·052. At the final stage of the refinement all the parameter shifts were less than one eighth of the corresponding standard deviations. Unit weight was adopted for all the reflexions. The same atomic scattering factors as those for the low-temperature phase were used. The final atomic parameters are given in Table 3.*

Description of the structure and discussion

Projections of the low- and high-temperature modifications along the a axis are shown in Fig. 1(a) and (b) respectively. The structures of both modifications are dominated by segregated stacks of $TCNQ^-$ anions along the a axis. Moreover, the structures form layers consisting of only $TCNQ^-$ anions and of only K^+ cations parallel to the (100) plane. An important difference between the two modifications lies in the stacking mode of the $TCNQ^-$ ions. In the low-temperature modification two crystallographically independent $TCNQ^-$ anions (I) and (II) form separate columns with alternating interplanar distances as shown in Table 4. Accordingly, dimeric $TCNQ^-$ units exist with an average interplanar distance of 3·237 Å. Above the transition temperature the $TCNQ^-$ ions slightly change the orientation around the dotted lines as illustrated in Fig. 1(a) and they are stacked with equal interplanar distances of 3·479 Å. Thus this is a monomer–dimer transition similar to that already reported for Na^+TCNQ^-.

* Lists of observed and calculated structure amplitudes for the two modifications have been deposited with the British Library Lending Division as Supplementary Publication No. SUP 32098 (19 pp.). Copies may be obtained through The Executive Secretary, International Union of Crystallography, 13 White Friars, Chester CH1 1NZ, England.

Table 3. *Atomic parameters for the high-temperature modification*

(a) Non-hydrogen coordinates and anisotropic temperature factors (×10⁴)

	x	y	z	U_{11}	U_{22}	U_{33}	U_{12}	U_{13}	U_{23}
K	5000	5000	0	512 (13)	532 (18)	483 (15)	−28 (13)	118 (10)	−13 (15)
C(1)	80 (19)	794 (7)	795 (7)	547 (48)	474 (68)	371 (53)	−42 (35)	−74 (31)	48 (41)
C(2)	519 (21)	1035 (8)	−280 (7)	751 (62)	396 (61)	406 (59)	−101 (39)	−56 (36)	109 (52)
C(3)	−525 (22)	−280 (7)	1032 (8)	812 (60)	378 (72)	519 (62)	−57 (37)	190 (38)	87 (47)
C(4)	21 (18)	1570 (7)	1582 (6)	565 (46)	498 (66)	428 (54)	−9 (36)	52 (35)	92 (49)
C(5)	−378 (20)	1330 (7)	2667 (8)	584 (50)	436 (58)	515 (65)	−24 (35)	−36 (39)	20 (48)
C(6)	422 (21)	2651 (8)	1341 (7)	693 (55)	423 (73)	601 (58)	12 (40)	210 (39)	18 (50)
N(1)	−658 (21)	1097 (7)	3507 (7)	1185 (68)	685 (67)	456 (63)	−50 (42)	119 (40)	−29 (52)
N(2)	680 (20)	3530 (7)	1135 (7)	1018 (61)	538 (70)	627 (57)	−46 (40)	208 (39)	23 (48)

(b) Hydrogen coordinates (×10³) and isotropic temperature factors

	x	y	z	B (Å²)
H(2)	56 (13)	164 (6)	−63 (5)	2·1 (1·5)
H(3)	−75 (13)	−47 (5)	178 (5)	1·7 (1·2)

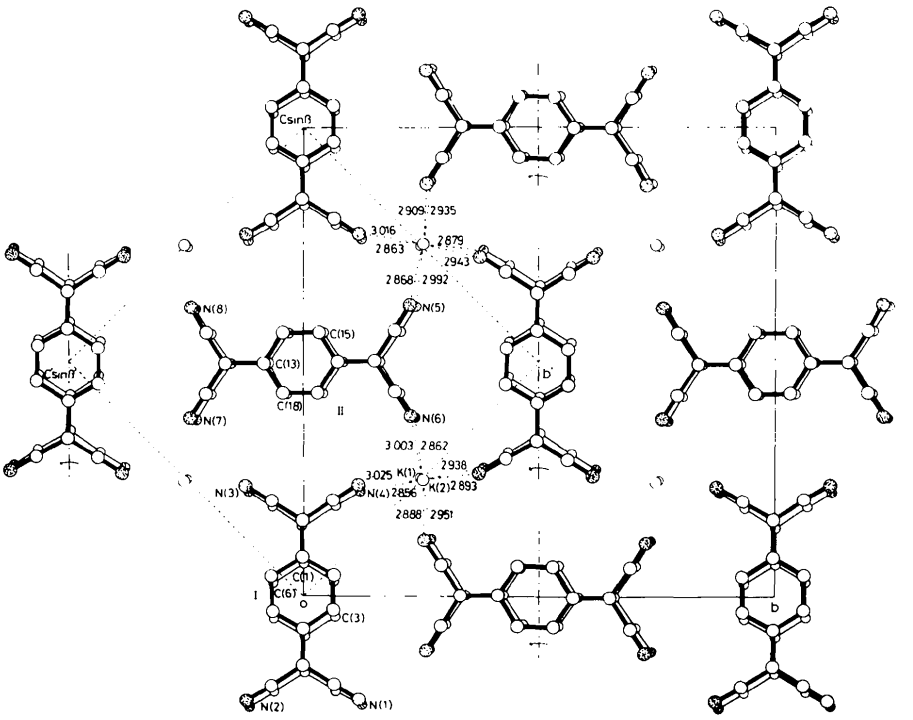

(*a*)

Fig. 1. Structures viewed along the *a* axis. (*a*) Low-temperature phase. The *b* and *c* axes of the high-temperature modification are drawn as broken lines.

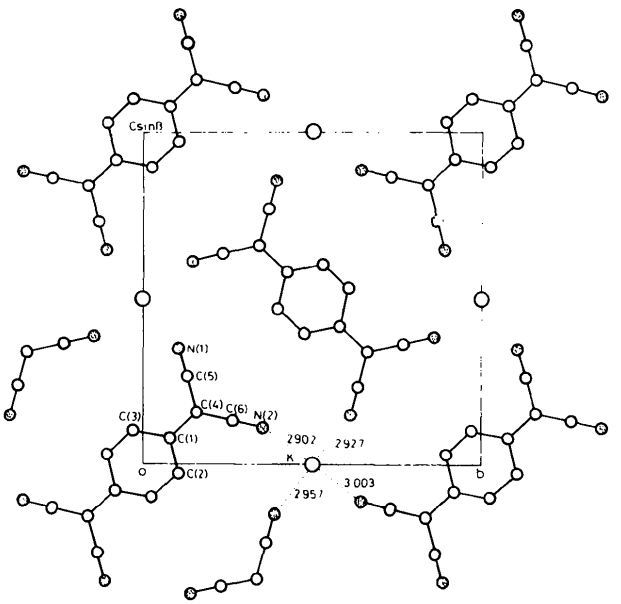

(*b*)

Fig. 1 (*cont.*). (*b*) High-temperature phase.

Interplanar distances between $TCNQ^-$ ions of the two modifications of Na^+TCNQ^- are also included in Table 4 for comparison. All the interplanar distances in the

Table 4. *Interplanar distances between $TCNQ^-$'s*

(*a*) Na^+TCNQ^-

	Low-temperature modification		High-temperature modification
	TCNQ (I)	TCNQ (II)	
In dimeric unit	3·223 Å	3·200 Å	3·385 Å
Between dimeric units	3·505	3·480	

(*b*) K^+TCNQ^-

	Low-temperature modification		High-temperature modification
	TCNQ (I)	TCNQ (II)	
In dimeric unit	3·240 Å	3·234 Å	3·479 Å
Between dimeric units	3·554	3·580	

K^+ salt are appreciably longer than in the Na^+ salt, which reflects the difference in ionic radii and co-ordination numbers of K^+ and Na^+.

In the low-temperature phase of the K^+ salt, $TCNQ^-$ (I) and (II) radicals are inclined at angles of 15·8 and 11·3° respectively to the plane (100). Above the transition temperature, the inclination angle reduces to 8·9°.

Fig. 2 shows the overlapping modes of adjacent $TCNQ^-$ units. In the low-temperature phase a modified ring–ring overlap with the shift of molecular centre

along its short axis is observed in the dimeric unit. Between dimeric units there is a modified ring–ring overlap with a diagonal shift of the molecular centre. In the high-temperature phase, however, there is a modified ring–ring overlap of a type intermediate between those observed in the low-temperature phase. The change in overlapping mode at the phase transition is the same as that observed in Na^+TCNQ^-.

A marked difference between the K^+ and Na^+ salts lies in the coordination of the cations. A K^+ ion is situated at the centre of a distorted cube consisting of eight N atoms of different $TCNQ^-$ radicals, whereas the Na^+ ion is coordinated octahedrally by six N atoms. Distances between K^+ ions and N atoms are in the range 2·856 to 3·025 Å with an average distance of 2·926 Å in the low-temperature modification, while they are 2·927, 2·957, 2·902 and 3·003 Å in the high-temperature modification.

In the low-temperature phase K^+ ions are arranged along the *a* axis with alternating distances of 3·539 and 3·550 Å. Above the transition temperature, they are arranged at an equal distance of 3·550 Å. Short contacts between the N atoms of adjacent $TCNQ^-$'s are compared in Table 5 for both modifications. Above the transition temperature, these distances increase and the electrostatic repulsive force between like charges decreases.

The molecular geometry is summarized in Fig. 3. No significant differences are observed between the two modifications. Estimated standard deviations of bond angles in the low- and high-temperature modifications are 0·4–0·5° and 0·8–1·1° respectively. Figures in parentheses give deviations from the least-squares plane of the quinoid skeleton, indicating that both $C(CN)_2$ residues of all the $TCNQ^-$ ions are slightly twisted around the long molecular axis on the same side. These features are the same as observed in Na^+TCNQ^- but different from the shallow boat form observed in Rb^+TCNQ^- (Hoekstra, Spoelder & Vos, 1972). The $C(CN)_2$ tail makes an average angle of 3·4° around the C=C bond with respect to the least-squares plane of the quinoid skeleton in the low-temperature phase which decreases to 2·5° in the high-temperature phase.

Structural change with temperature

Unit-cell dimensions were determined in the temperature range 30 to 140°C by least-squares calculations on the basis of eight 2θ values measured on an automatic four-circle diffractometer. The temperature dependence of the unit-cell volume is presented in Fig. 4, where four times the volume of the high-temperature modification is plotted for convenience. With a rise in temperature the volume increases continuously. The extrapolation of the curve towards the transition temperature shows that there is little, if any, discontinuity at the transition temperature *Tc*. The volume of the

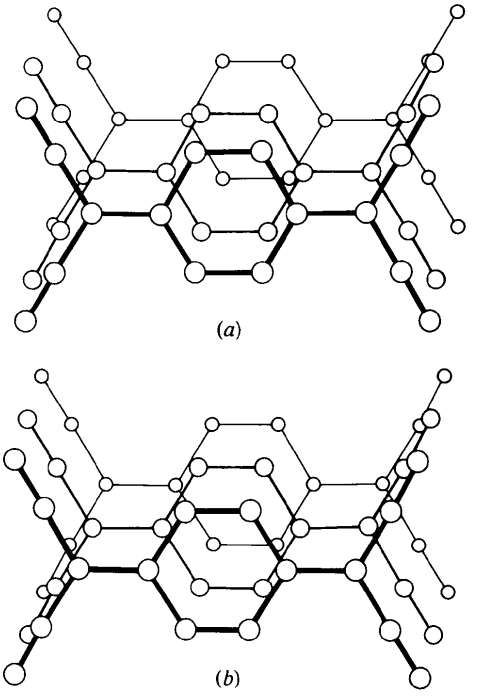

Fig. 2. Overlapping modes of adjacent $TCNQ^-$ units. (*a*) Low-temperature phase. (*b*) High-temperature phase.

Table 5. *Short contacts* (Å) *between the* N *atoms of adjacent* $TCNQ^-$*'s*

(*a*) Low-temperature phase

Symmetry code

(i)	x,	y,	z	(vi)	$\frac{1}{2}+x$, $\frac{1}{2}-y$, $-\frac{1}{2}+z$
(ii)	$\frac{1}{2}-x$,	$\frac{1}{2}+y$,	$\frac{1}{2}-z$	(vii)	$-x$, $-y$, $-z$
(iii)	$1-x$,	$-y$,	$-z$	(viii)	$-x$, $-y$, $1-z$
(iv)	$1-x$,	$-y$,	$1-z$	(ix)	$-\frac{1}{2}+x$, $\frac{1}{2}-y$, $\frac{1}{2}+z$
(v)	$\frac{1}{2}+x$,	$\frac{1}{2}-y$,	$\frac{1}{2}+z$	(x)	$-\frac{1}{2}+x$, $\frac{1}{2}-y$, $-\frac{1}{2}+z$
				(xi)	$-1+x$, y, z

$N(4^i)\cdots N(6^i)$	3·339 (6)	$N(2^{iii})\cdots N(8^{iv})$	3·269 (6)
$N(6^i)\cdots N(3^{ii})$	3·237 (6)	$N(8^{iv})\cdots N(1^v)$	3·370 (6)
$N(3^{ii})\cdots N(7^{ii})$	3·275 (6)	$N(1^v)\cdots N(5^{vi})$	3·286 (6)
$N(7^{ii})\cdots N(4^i)$	3·273 (6)	$N(5^{vi})\cdots N(2^{iii})$	3·294 (6)
$N(4^i)\cdots N(2^{iii})$	3·451 (7)	$N(4^i)\cdots N(2^{vii})$	3·640 (7)
$N(6^i)\cdots N(8^{iv})$	3·454 (7)	$N(6^i)\cdots N(8^{viii})$	3·635 (7)
$N(3^{ii})\cdots N(1^v)$	3·440 (7)	$N(3^{ii})\cdots N(1^{ix})$	3·651 (7)
$N(7^{ii})\cdots N(5^{vi})$	3·458 (7)	$N(7^{ii})\cdots N(5^x)$	3·638 (7)

(*b*) High-temperature phase

Symmetry code

(i)	x,	y,	z	(iii)	$-x$, $\frac{1}{2}+y$, $\frac{1}{2}-z$
(ii)	x,	$\frac{1}{2}-y$,	$\frac{1}{2}+z$	(iv)	$1+x$, y, z

$N(2^i)\cdots N(1^{ii})$	3·331 (12)	$N(2^i)\cdots N(1^{iii})$	3·286 (13)
$N(1^i)\cdots N(1^{iv})$	3·587 (16)		

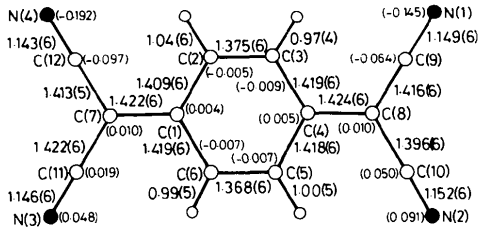

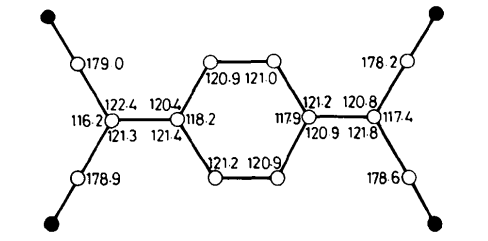

(*a*)

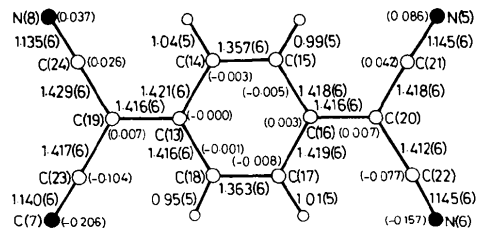

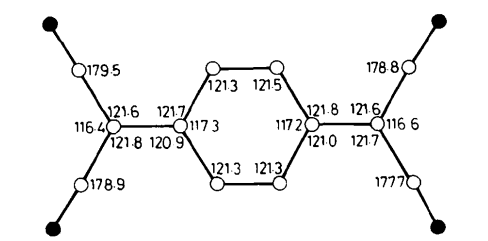

(*b*)

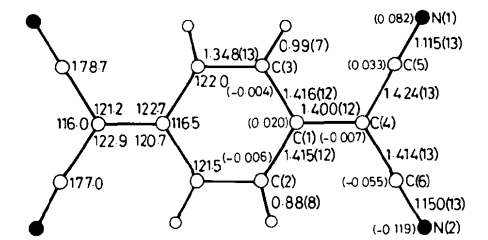

(*c*)

Fig. 3. Bond distances (Å) and bond angles (°) in $TCNQ^-$ residues with the standard deviations. The numbers in parentheses are the atomic displacements from the least-squares plane of the quinodimethane moiety. (*a*) $TCNQ^-$ (I) in the low-temperature phase. (*b*) $TCNQ^-$ (II) in the low-temperature phase. (*c*) $TCNQ^-$ in the high-temperature phase.

high-temperature phase increases more slowly than that of the low-temperature phase. The temperature variations of $\Delta a/a_{30}$, $\Delta b/b_{30}$, $\Delta c/c_{30}$ and β are illustrated in Fig. 5, where a_{30} *etc.* stand for the lattice constants at 30°C. A remarkable elongation along the *a* axis is observed, indicating the expansion along $TCNQ^-$ columns.

The temperature dependences of the intensities of an even reflexion, 200, and a strong uneven reflexion, 310, were measured. 200 of the low-temperature phase changes into the corresponding 100 of the high-temperature phase. The intensity of 200 (and of 100)

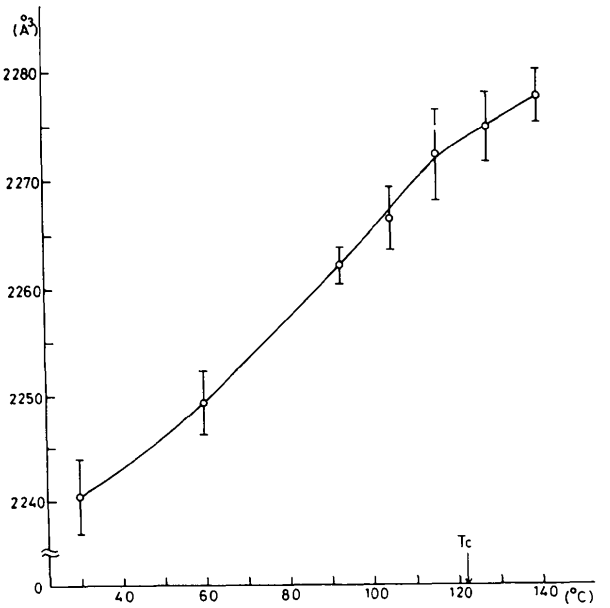

Fig. 4. The temperature dependence of the unit-cell volume.

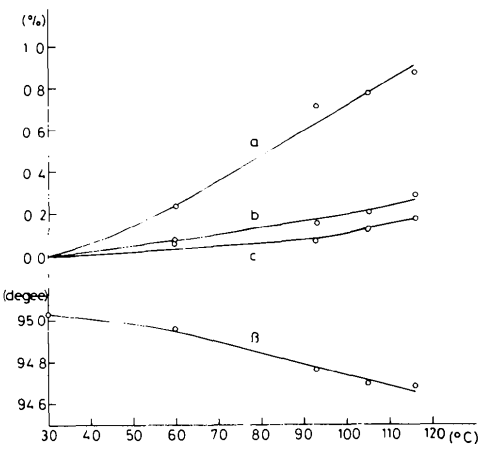

Fig. 5. The temperature variations of $\Delta a/a_{30}$, $\Delta b/b_{30}$, $\Delta c/c_{30}$ and β angle in the low-temperature phase where a_{30} *etc.* stand for the lattice constants at 30°C.

remains almost unaltered over the measured temperature range. The intensity of 310 is proportional to $(\mathbf{H}.\Delta\mathbf{r})^2$ in the same way as described in the previous paper (Konno & Saito, 1975), where $\mathbf{H}$ is the reciprocal lattice vector and $\Delta\mathbf{r}$ stands for the displacement of the molecular centre of TCNQ from the monomeric 'average structure'. The ratio of the structure factor of the 310 reflexion to that at 30°C is shown in Fig. 6. The structure factor of 310 decreases as the temperature is raised, and drops suddenly to zero at 122°C. This rapid decrease indicates the decrease in $\Delta\mathbf{r}$ and suggests that the $TCNQ^-$ already starts to shift in the column at 30°C. With a rise in temperature the interplanar distances in the dimeric units increase gradually and those between dimeric units decrease to approach more closely a monomeric structure. However, the monomeric structure does not materialize until the transition temperature is attained. The transition accompanies hysteresis. The observed temperature of the phase transition in the heating direction was higher by about 6°C than that in the cooling direction, which suggests a first-order phase transition.

Crystals of alkali$^+$ $TCNQ^-$ undergo an insulator–insulator transition (Vegter, Hibma & Kommandeur, 1969; Sakai, Shirotani & Minomura, 1972*a*,*b*). The magnetic properties of these salts with low or intermediate electrical conductivity have been explained mainly by an antiferromagnetic Heisenberg model or a tight-binding band model (Kepler, 1963; Khanna, Bright, Garito & Heeger, 1974; Vegter, Kuindersma & Kommandeur, 1971; Hibma & Kommandeur, 1975).

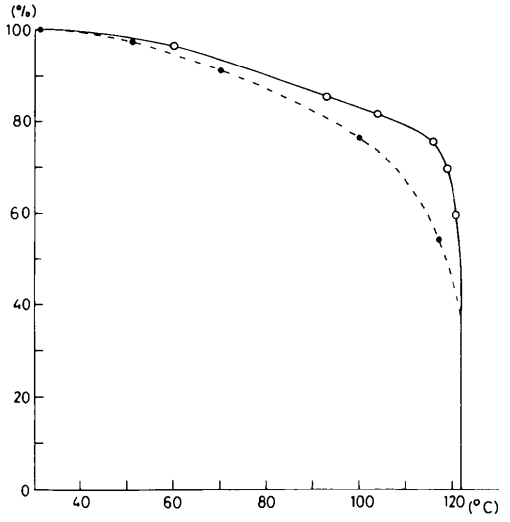

Fig. 6. The temperature dependence of ξ_T/ξ_{303} estimated from the structure-factor ratio $F(310)_T/F(310)_{303}$ (——) and $\sqrt{\{(\chi_{Tc}Tc-\chi_T T)/[\chi_{Tc}Tc-\chi_{303}(303)]\}}$ (——)

An attempt has been made to correlate the observed structural change in the TCNQ columns with the temperature dependence of the magnetic susceptibility, on the basis of the Heisenberg model. In crystals of alkali$^+$ $TCNQ^-$ salts the ground state is greatly stabilized with respect to its triplet exciton state owing to the correlation with the charge-transfer state. The stabilization energy J depends on the square of the overlap integral between the half-filled highest orbitals of adjacent $TCNQ^-$'s (Oohashi & Sakata, 1973). Let us consider a centrosymmetric chain consisting of $2N$ $TCNQ^-$'s with alternating spacings of $r(1-\zeta)$ and $r(1+\zeta)$, where $\zeta(\equiv\Delta r/r)$ is a parameter to describe the dimeric structure and r is the distance between the $TCNQ^-$'s in the 'average structure'. It can easily be shown that J may be approximately written as: $J=-(\epsilon_0+\frac{1}{2}\epsilon_2\zeta^2)$, where ϵ_0 and ϵ_2 are constants. This gain in the electronic energy due to the formation of the dimeric structure is balanced by the increase in column distortion energy at absolute zero. Since the columnar structure is centrosymmetric, odd-order terms of ζ in the expansion of the column distortion energy vanish and the following expression may be obtained: $\frac{1}{2}g_2\zeta^2+\frac{1}{4}g_4\zeta^4$, where g_2 and g_4 are constants. With increasing temperature, loss of stabilization energy arising from thermal excitation leads to less column distortion. If the interaction between the triplet excitons is neglected, the free energy of the system can be given in terms of the density of the triplet state, ρ, as follows

$$F/N = -[\epsilon_0+\tfrac{1}{2}\epsilon_2\zeta^2](1-\rho)+\tfrac{1}{2}g_2\zeta^2+\tfrac{1}{4}g_4\zeta^4 - kT[\rho\ln 3-\rho\ln\rho-(1-\rho)\ln(1-\rho)] \quad (1)$$

where the last term stands for the entropy due to the triplet excitons in a system of $2N$ $TCNQ^-$'s with the dimeric structure (Chesnut, 1964). From the requirement imposed by the equilibrium-state condition: $\delta F/\delta\zeta=0$ and $\delta F/\delta\rho=0$, we have

$$\zeta=0 \quad \text{or} \quad \zeta^2=[\epsilon_2(-\rho)-g_2]/g_4 \quad (2)$$

and

$$\rho=\{1+\tfrac{1}{3}\exp[(\epsilon_0+\tfrac{1}{2}\epsilon^2)/(kT)]\}^{-1}. \quad (3)$$

If $\epsilon_2(1-\rho)>g_2$, we obtain a value of ζ different from zero for the distortion. With an increase in ρ, ζ decreases and reduces to zero at the transition temperature, Tc. Accordingly we have $g_2=\epsilon_2(1-\rho_{Tc})$. Inserting this relation into equation (2), we find that

$$\zeta=\sqrt{(\epsilon_2/g_4)(\rho_{Tc}-\rho_T)}. \quad (4)$$

The paramagnetic susceptibility χ for the dimeric structure with the triplet exciton state is represented by

$$\chi = \frac{g^2\beta^2 N}{3kT}\rho, \tag{5}$$

where g is the electronic g factor and is equal to 2·00, β is the Bohr magneton and N is Avogadro's number. From equations (4) and (5), the column distortion is associated with the magnetic susceptibility in the following way,

$$\frac{\xi_T}{\xi_{303}} = \sqrt{\frac{\rho_{Tc}-\rho_T}{\rho_{Tc}-\rho_{303}}} = \sqrt{\frac{\chi_{Tc}Tc-\chi_T T}{\chi_{Tc}Tc-\chi_{303}(303)}} \tag{6}$$

In Fig. 6 the ξ_T/ξ_{303}, estimated from $F(310)_T/F(310)_{303}$, are compared with those obtained from experimental magnetic susceptibilities by means of equation (6) (Vegter *et al.*, 1969). In spite of the rather crude approximation, the two curves are similar. For further improvement, the interaction between triplet exciton states and the effect of expansion of the column with temperature should be considered.

The fact that this transition is first order and the crystal structure changes at the transition temperature indicates that the interaction between K^+ and $TCNQ^-$, as well as the interaction between the columns, plays an important role.

The computations were performed on the FACOM 270-48 at this Institute with a local version of the *Universal Crystallographic Computation Program System, UNICS* (1967). Part of the cost of this research was met by a Scientific Research Grant from the Ministry of Education, to which the authors' thanks are due.

References

ANDERSON, G. R. & FRITCHIE, C. J. (1963). Second National Meeting, Society for Applied Spectroscopy, San Diego, October 14–18, paper 111.

BOER, J. L. DE & VOS, A. (1972). *Acta Cryst.* B**28**, 839–848.

CHESNUT, D. B. (1964). *J. Chem. Phys.* **40**, 405–411.

COMÈS, R., LAMBERT, M., LAUNOIS, H. & ZELLER, H. R. (1973). *Phys. Rev.* B**8**, 571–575.

DENOYER, F., COMÈS, F., GARITO, A. F. & HEEGER, A. J. (1975). *Phys. Rev. Lett.* **35**, 445–449.

HIBMA, T. & KOMMANDEUR, J. (1975). *Solid State Commun.* **17**, 259–262.

HOEKSTRA, A., SPOELDER, T. & VOS, A. (1972). *Acta Cryst.* B**28**, 14–25.

International Tables for X-ray Crystallography (1962). Vol. III, 2nd ed. Birmingham: Kynoch Press.

KEPLER, R. G. (1963). *J. Chem. Phys.* **39**, 3528–3532.

KHANNA, S. K., BRIGHT, A. A., GARITO, A. F & HEEGER, A. J. (1974). *Phys. Rev.* B**10**, 2139–2143.

KONNO, M. & SAITO, Y. (1974). *Acta Cryst.* B**30**, 1294–1299.

KONNO, M. & SAITO, Y. (1975). *Acta Cryst.* B**31**, 2007–2012.

OOHASHI, Y. & SAKATA, T. (1973). *Bull. Chem. Soc. Japan*, **46**, 3330–3335.

SAKAI, N., SHIROTANI, I. & MINOMURA, S. (1972*a*). *Bull. Chem. Soc. Japan*, **45**, 3314–3320.

SAKAI, N., SHIROTANI, I. & MINOMURA, S. (1972*b*). *Bull. Chem. Soc. Japan*, **45**, 3321–3328.

STEWART, R. F., DAVIDSON, E. R. & SIMPSON, W. T. (1965). *J. Chem. Phys.* **42**, 3175–3187.

UNICS (1967). Edited by T. SAKURAI. Tokyo: The Crystallographic Society of Japan.

VEGTER, J. G., HIBMA, T. & KOMMANDEUR, J. (1969). *Chem. Phys. Lett.* **3**, 427–429.

VEGTER, J. G., KUINDERSMA, P. I. & KOMMANDEUR, J. (1971). *Conduction in Low-Mobility Materials*, edited by N. KLEIN, D. S. TANNHAUSER & M. POLLAK, pp. 363–373. London: Taylor and Francis.